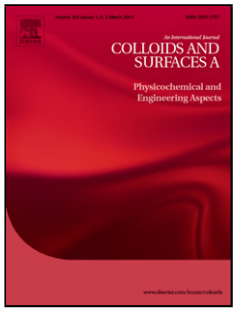

Title: The self-association equilibria of doxorubicin at high concentration and ionic strength characterized by fluorescence spectroscopy and molecular dynamics simulations

Authors: Elisamaria Tasca, Josephine Alba, Luciano Galantini, Marco D'Abramo, Anna Maria Giuliani, Andrea Amadei, Gerardo Palazzo, Mauro Giustini

PII: S0927-7757(19)30169-4
DOI: https://doi.org/10.1016/j.colsurfa.2019.06.005
Reference: COLSUA 23539

To appear in: *Colloids and Surfaces A: Physicochem. Eng. Aspects*

Received date: 27 February 2019
Revised date: 29 May 2019
Accepted date: 3 June 2019

Please cite this article as: Tasca E, Alba J, Galantini L, D'Abramo M, Giuliani AM, Amadei A, Palazzo G, Giustini M, The self-association equilibria of doxorubicin at high concentration and ionic strength characterized by fluorescence spectroscopy and molecular dynamics simulations, *Colloids and Surfaces A: Physicochemical and Engineering Aspects* (2019), https://doi.org/10.1016/j.colsurfa.2019.06.005

The self-association equilibria of doxorubicin at high concentration and ionic strength characterized by fluorescence spectroscopy and molecular dynamics simulations

Elisamaria Tasca[a,#], Josephine Alba[a,#], Luciano Galantini[a,b], Marco D'Abramo[a], Anna Maria Giuliani[c], Andrea Amadei[d], Gerardo Palazzo[e,b*], Mauro Giustini[a,b**]

[a]Chemistry Department, University "La Sapienza", P.le Aldo Moro 5, 00185 Roma (Italy)

[b]Centre for Colloid and Surface Science - C.S.G.I. Operative Unit of Bari c/o Chemistry Department, University "Aldo Moro", Bari (Italy)

[c]STEBICEF Department, University of Palermo, Palermo (Italy)

[d]Science and Chemical Technology Department, University of Tor Vergata, Roma (Italy)

[e]Chemistry Department, University "Aldo Moro", Bari (Italy)

[#]These Authors contributed equally to this work.

Corresponding authors: *gerardo.palazzo@uniba.it; **mauro.giustini@uniroma1.it

Graphical abstract

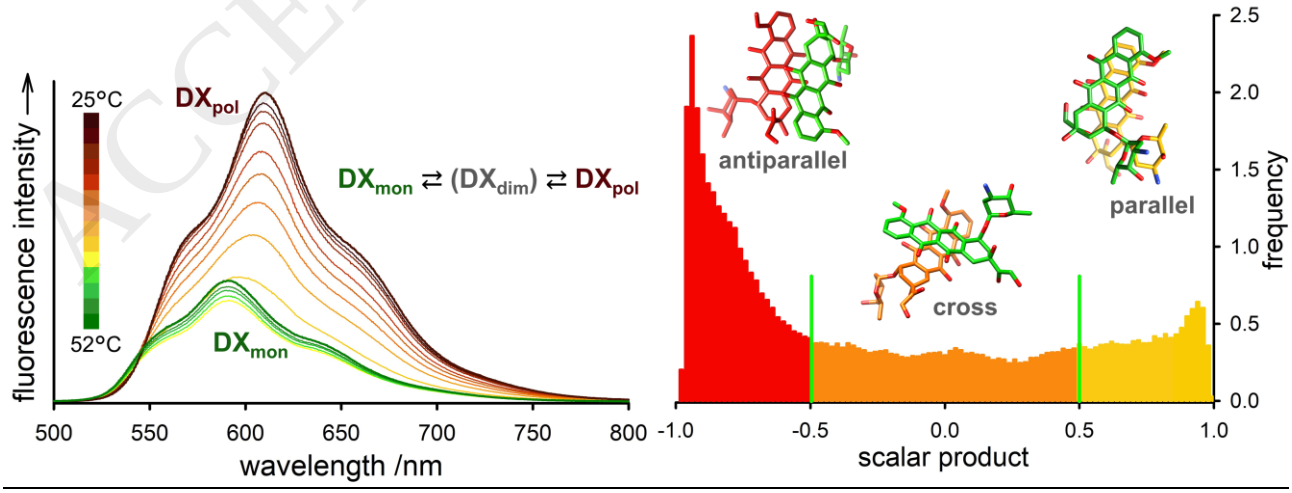

ABSTRACT

The self-association equilibria of doxorubicin hydrochloride (DX), at high drug and NaCl concentrations, are studied by temperature scan fluorescence spectroscopy, with the support of molecular dynamics (MD) calculations.
Even though all anthracyclines show dimerization equilibria, DX only can further associate into long polymeric chains according to $DX_{mon} \rightleftarrows DX_{dim} \rightleftarrows DX_{pol}$.
This is reflected not only in the mechanical properties of DX_{pol} solutions (behaving as thixotropic gels) but also in their spectroscopic behaviour. Fluorescence, in particular, is the technique of election to study this complex set of equilibria. Upon increasing the temperature, DX_{pol} melts into DX_{dim}, which in turn is in equilibrium with DX_{mon}. Since DX_{dim} is non fluorescent, with a fluorescence temperature scan experiment the $DX_{pol} \rightleftarrows DX_{mon}$ equilibrium is probed. However, also information on the DX dimerization equilibrium can be derived together with the relevant thermodynamic parameters ruling the dimerization process ($\Delta H^{\circ}_{dim} = -56\ \mathrm{kJ\ mol^{-1}}$; $\Delta S^{\circ}_{dim} = -97\ \mathrm{J\ mol^{-1}\ K^{-1}}$). The residence time of DX molecules in the dimer (74.7 μs), as well as the monomers mutual orientation in the dimer, are characterized by means of theoretical and computational modelling.

Keywords

Fluorescence Spectroscopy; Molecular Dynamics; Doxorubicin; Self-Association

Introduction

The anticancer antibiotic doxorubicin hydrochloride (DX – Chart 1) is a powerful drug used for the treatment of several malignancies. The first trials with doxorubicin (at that time named adriamycin) started back in 1969; thereafter the drug was approved for clinical use with exceptional results in spite of the many toxic side-effects[1] and the development of multidrug resistance.[2] Very active research started very soon to try to overcome these drawbacks, and it is still alive, trying to find new formulations or new administration strategies.[1][3][4]

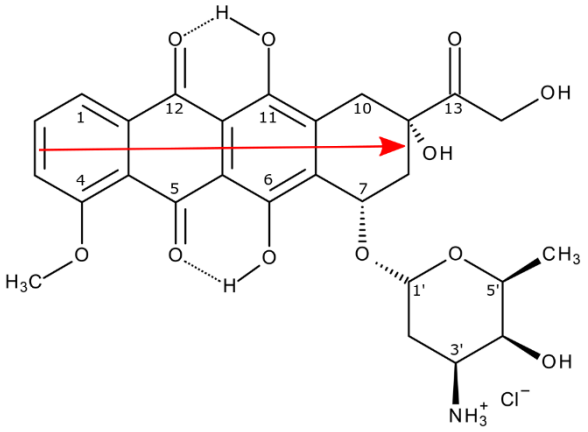

Chart 1 Doxorubicin hydrochloride (DX) chemical structure. The red arrow indicates the long axis of the molecule.

From a physico-chemical point of view, DX is an extremely intriguing molecule. Despite its relatively low molar mass (580 g/mol), it exhibits features typical of high molecular weight species, such as the capability to act as a water gelator. This feature has been described in several papers back in the nineties[5][6][7][8] and has recently been the subject of a deep investigation that revealed the peculiar association of DX molecules into supramolecular aggregates made of hundreds of units (distorted dimers).[9] Interestingly, the closely related molecule epirubicin hydrochloride, that differs from DX only for the stereochemistry at the C4' carbon atom in the aminosugar moiety of the drug, does not form gels in the same conditions that induce DX gelling. Molecular dynamics simulations revealed that this was due to the critical network of hydrogen bonds holding together the supramolecular assembly of DX in the gels, possible only for the specific stereochemistry of donors and acceptors fulfilled in the DX molecule.[9] The stereochemically driven supramolecular polymerization of DX is a consequence of the capacity of DX to form dimers in solution, even though the gelification is not just the extension to many molecules of the dimerization process. In fact, dimerization is a characteristic shared by all anthracyclines,[10] while gelification, as already said, is a DX peculiarity.

Self-association of anthracyclines has been the subject of several investigations, [11][12][13][14][15] however an analysis of the all set of DX association equilibria by means of fluorescence spectroscopy, is not present, to our knowledge, in the literature.

Among anthracyclines, DX is the only molecule, so far, to show a complex pattern of self-association equilibria that goes beyond the classical monomer ⇄ dimer equilibrium. When the analytical concentration exceeds the Critical Gel Formation Concentration (CGFC),[8] even in the absence of salts, as we recently demonstrated,[9] the complete set of equilibria

$$DX_{mon} \rightleftarrows DX_{dim} \rightleftarrows DX_{pol}$$

has to be taken into account to properly describe the DX solutions behaviour.

In the present study an extension of the analysis of the association equilibria of DX leading to its polymerization into gels will be presented exploiting the joint use of fluorescence spectroscopy, theoretical modelling and Molecular Dynamics (MD) simulations. In addition, the thermodynamic properties of these equilibria have been characterized. It has to be pointed out, finally, that only at high DX concentration and in the presence of salt the supramolecular DX polymerization leading to gels occurs, making thus possible to probe the whole set of association equilibria above introduced.

Materials and Methods

Doxorubicin hydrochloride was a kind gift of Farmitalia Carlo-Erba Chem. Co. All the other chemicals used, of the highest available purity, were from Sigma-Aldrich. Ultrapure water (18.2

MΩ/cm) from Arium pro UV system (Sartorius Stedim Biotech) was used in the preparation of the solutions.

Samples were prepared by diluting a 0.02M solution of DX with suitable amounts of 5M NaCl stock solution and water directly into a 1.5 mL Eppendorf vial to obtain the final DX concentration of 0.01M and the desired final NaCl concentration. Samples were vortex mixed for several minutes and then centrifuged at 1500 r.p.m. (Hettich Mikro 20). They were left to equilibrate in the dark at room temperature for 30 minutes before transferring them into the cuvette for the spectroscopic measurements.

Steady-state fluorescence measurements were performed on a Fluoromax 2 instrument (Horiba-Jobin Yvon), equipped with a Peltier thermostatted *LUMA 40/JY1* sample holder (Quantum Northwest) controlled by the TC1 unit via the T-App software from the same manufacturer. Sample temperature was measured through a QNW-1 thermistor probe located in close proximity of the 0.01 cm sandwich cells (Hellma) used, directly connected to the TC-1 unit (accuracy: ± 0.01°C). The cell was oriented at 45° respect to the exciting beam (angular geometry) paying attention to avoid direct reflection reaching the emission monochromator. Temperature was varied using a ramp temperature of 0.5 °C/min and once reached the target temperature, the sample was left for further 4 min to ensure thermal equilibration. Samples were excited at 410 nm and the excitation and emission slits were both set at 2.5 nm; integration time was 0.25 s and spectra were acquired in the 500-800 nm region, with a step of 0.5 nm.

The temperature range explored along fluorescence T-scan experiments broadly covered the interval 293-328 K, depending on samples.

The all-atoms MD simulations were performed using the Gromacs software package version 2018.1 [16] on two DX molecules solvated in a cubic box using the SPC water model. [17] The force field for DX, successfully used in our previous work [9] and obtained from the ATB server, is derived using a multistep process in which results from quantum mechanical calculations are combined with a knowledge-based approach to ensure compatibility with a specific parameter set of well-known force fields.[18] After thermalization, an equilibration phase of 10 ns has been performed to let the systems reach their local minimum. Then, two MD simulations of two DX molecules in water (at 300K and 450K lasting 200 ns each) were performed in the canonical ensemble (NVT) with periodic boundary conditions and using the v-rescale temperature coupling.[19]

The temperature of 450 K has been chosen after a sensitivity analysis obtained by short MD simulations in the interval between 300 K and 500 K. Such data indicate that the temperature of 450 K guarantees the sampling of a significant number of monomer-dimer transitions in a reasonable amount of time (vide infra).

Following our previous works,[20][21] the box volume (~ 91 nm^3) at each temperature has been tuned to reproduce the pressure of 560 bar, the value at which the SPC model has a density corresponding to liquid water, i.e. 55.32 mol/L.[20] In this way the solute-solvent systems could be considered as inserting a solute into a solvent box at the same temperature and pressure of the reference solvent box, thus mimicking the experimental conditions of solvating a solute into liquid water. The bonds were constrained by means of the LINCS algorithm[22] and the particle mesh Ewald method[23] was used to compute long range interactions. A cut-

off of 1.1 nm was used. The atomic coordinates were written every 2 ps and all the analyses have been performed on 50000 frames.

Results and Discussion

Fluorescence Spectroscopy

All anthracyclines and DX in particular, are fluorescent molecules (the fluorescence quantum yield of the DX monomer is $\Phi_{DX}^{mon} = 3.9 \cdot 10^{-2}$)[9] but their fluorescence dramatically drops upon dimerization $\left(\Phi_{DX}^{dim} \approx 10^{-5}\right)$.[24]

When above a critical concentration of both the drug and NaCl (the so called CGFC [8]), the DX solutions turn into gels and we have shown that this process is due to a supramolecular polymerization of DX in a two-state process between the gel and dimers, leading to the formation of DX_{pol}.[9] The fluorescence spectrum of DX_{pol} is markedly different from that of DX_{mon} and since the DX supramolecular polymerization is a T-controlled process, upon heating a DX_{pol} sample, due to the non-fluorescent nature of DX_{dim}, the formation of only DX_{mon} was probed (even though CD spectroscopy revealed that DX_{pol} melts into DX_{dim} solution).[9]

Several deep investigations on anthracyclines dimerization process can be found in the literature and a spread of values for the relevant dimerization constant (K_{dim}) is reported. At 25 °C, literature values for K_{dim} of anthracyclines are in the range 10^3-10^5 M^{-1}, depending on ionic strength, buffer and experimental technique used, and decrease with temperature.[11][12][13][14][15][24][25] In the case of DX_{pol} samples, upon increasing the temperature, since they melt into non fluorescent dimers, a decrease in the fluorescence intensity is firstly observed followed by a shift in the maximum emission wavelength ($\lambda_{max}^{DX_{pol}} = 610$ nm; $\lambda_{max}^{DX_{mon}} = 495$ nm) and an increase of the fluorescence intensity. This feature can be appreciated in Figure 1 – Panel A where the spectra evolution with temperature of a DX_{pol} sample is shown. Along a fluorescence temperature scan experiment, therefore, it is the equilibrium $DX_{pol} \rightleftarrows DX_{mon}$ that is probed.

By considering the DX_{pol} emission spectrum acquired at low temperature as due only to polymerized DX molecules, and that at the highest temperature as due only to DX_{mon}, we can fit the intermediate emission spectra as the weighted sum of these two limiting spectra, i.e. E_{pol} and E_{mon}, according to

$$E_{(T)} = \chi_{pol} E_{pol} + \phi_{mon} E_{mon}$$

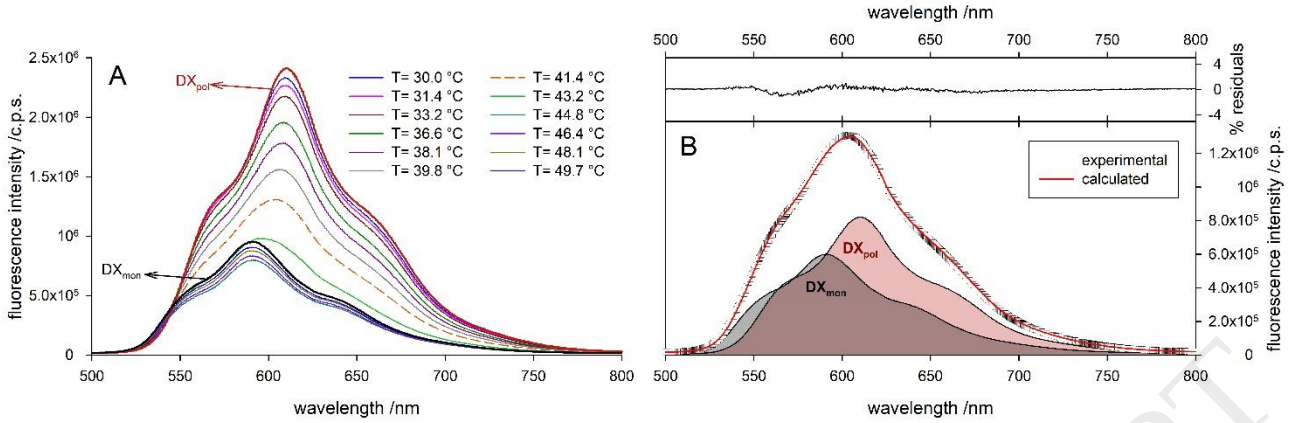

Figure 1 A) Fluorescence emission spectra as a function of temperature (see legend) for a DX_{pol} sample. The spectra acquired at temperatures between 52.0 °C (DX_{mon}; thick black line) and 25.0 °C (DX_{pol}; thick red line) have been fitted according to the procedure described in the text, to obtain the weight with which the two limit spectral shapes contribute to each intermediate spectrum. **B**) Example of the results obtained with such a procedure for the 41.4°C spectrum (dashed orange line in panel A) showing the weighted contribution of the two limit spectra (shaded spectra; χ_{pol}= 0.34 and ϕ_{mon}= 0.63) and the relevant percentage residuals (upper panel). $[DX]_{anal}$= 1·10^{-2} M; [NaCl]= 0.50 M.

An example of the results obtained is in Figure 1 – Panel B. While the weight factor for DX_{pol} is the true molar fraction of polymerized DX (χ_{pol}; at low temperature and in the presence of salt all the DX molecules are in the form of polymer, as evidenced by time resolved fluorescence data[9]), that of DX_{mon} is only the fraction (ϕ_{mon}) with which the spectral shape of DX_{mon} contributes to the total fluorescence emission spectrum at a certain temperature (i.e. $\phi_{mon} \propto \chi_{mon}$). In the case of DX samples at the very same concentration but without NaCl, upon increasing the temperature, the fluorescence intensity linearly increases since, as already said, in this situation only the $DX_{dim} \rightleftarrows DX_{mon}$ equilibrium is active and it moves to the right upon heating the solution. By assuming that at the highest probed temperature (52-53 °C, depending on samples) all the drug is in monomeric form, a normalization of all the spectra for this one allowed the weight factor of the DX_{mon} in the absence of salt to be calculated. In Figure 2 the result of these data treatment is summarized and it is evident that once DX_{pol} turned into a DX_{mon}+DX_{dim} solution, the systems behaviour is salt independent (all the ϕ_{mon} data coming from fluorescence emission spectra calculated at [NaCl]≠ 0.00 M lie on the data obtained at [NaCl]= 0.00 M). From the data in the absence of salt, the proportionality constant between ϕ_{mon} and χ_{mon} can be calculated since K_{dim} is known from the literature. By taking one of the literature data for the DX dimerization constant ($K_{dim}^{298\,K} = 6.3 \cdot 10^4\ M^{-1}$),[25] the true value of DX_{mon} molar fraction at 298K can be calculated thus allowing to solve the relation $\phi_{mon} = \kappa \cdot \chi_{mon}$.

The proportionality constant κ will depend only on the different fluorescence quantum yields of the species present in the system and on instrumental parameters. As long as the DX concentration and the acquisition parameters remain the same, it is possible to compare fluorescence measurements obtained at different salt concentrations thus calculating the

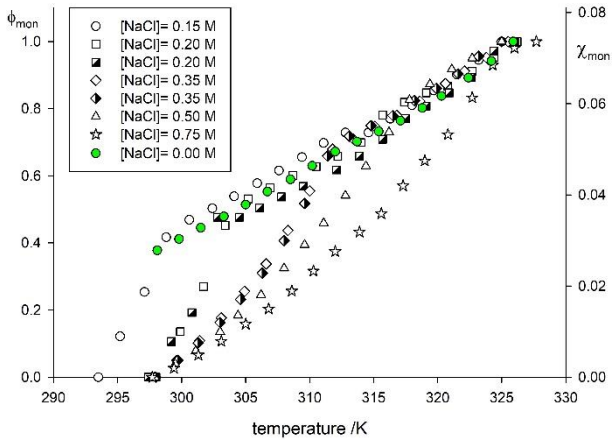

Figure 2 DX_{mon} weight factor (ϕ_{mon} – left hand axis) and the calculated true χ_{mon} values (κ= 13.59; right hand axis) as a function of temperature for DX samples at different salt content (see legend). [DX]= 1·10^{-2} M.

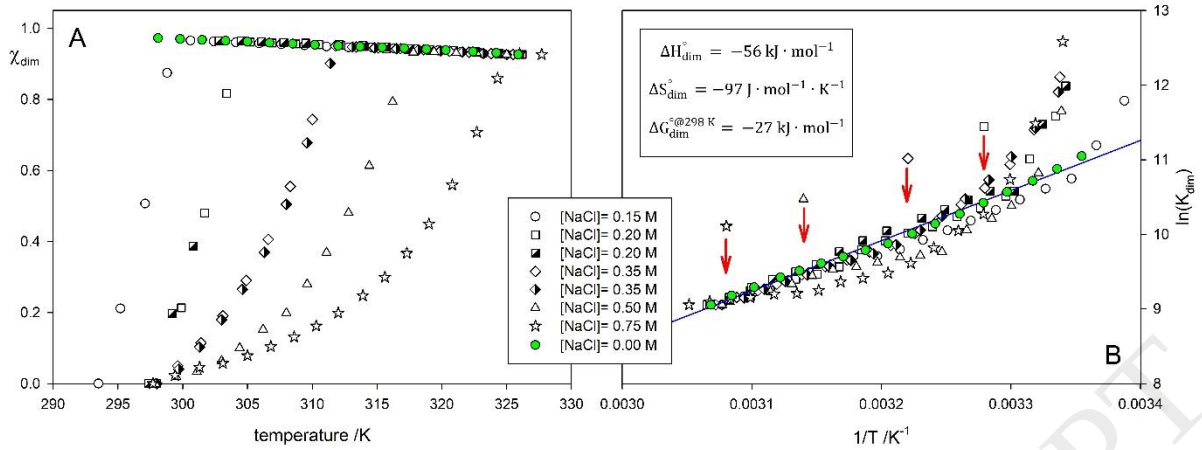

Figure 3 A) χ_{dim} values calculated from fluorescence spectra according to the procedure described in the text for DX concentrations above the CGFC in the absence (green points) and in the presence of NaCl (see legend). **B**) Van't Hoff plot for K_{dim} calculated from the χ_{mon} and χ_{dim} values obtained according to the procedure described in the text (same symbols as in panel **A**). Red arrows indicate the position of $1/T_{pol}$ (T_{pol} values taken from ref. [9]) for the different samples (see text for details).

true χ_{mon} values at all NaCl contents by simply dividing the ϕ_{mon} values by the instrumental constant κ (Figure 2 – right hand axis).

Since both χ_{pol} and χ_{mon} are known thank to the above described procedure, it is straightforward to calculate the χ_{dim} as 1-(χ_{mon} + χ_{pol}). Even though the presence of NaCl is fundamental for the DX polymerization into gels, once they are melted there is no dependence of χ_{dim} on NaCl concentration (Figure 3 – panel A). At this point the composition of the investigated systems along temperature scan experiments is known and this allows the relevant dimerization constant of DX to be calculated according to

$$K_{dim} = \frac{\chi_{dim}}{2[DX]_{anal} \cdot \chi^2_{mon}}$$

where χ_{dim} and χ_{mon} are the molar fractions of dimer and monomer DX, respectively and $[DX]_{anal}$ is the analytical concentration of the drug. At $[DX]_{anal}= 1\cdot10^{-2}$ M used throughout this work, at variance with literature reports,[10][12] even in the presence of NaCl there is no dependence of the dimerization constant on the ionic strength (Figure 3 – Panel B). This last point requires a few words of comment. It is evident that the K_{dim} values calculated from DX_{pol} samples lie on the same straight line of the sample without NaCl if two conditions are satisfied: *i*) the temperature is above T_{pol} (T_{pol} is the temperature at which the DX polymerization process starts upon cooling[9]); *ii*) the χ_{dim} values are not too small due to the high value of χ_{pol} (high uncertainty in the determination of the system composition due to the prevalence of DX_{pol}). Due to these reasons, at high NaCl concentrations and at low temperatures, deviations from the Van't Hoff prediction were observed (Figure 3 – panel B; the red arrows indicate the $1/T_{pol}$ values at the different NaCl concentrations, that correspond to: T_{pol}@0.75 M NaCl= 325 K; T_{pol}@0.50 M NaCl= 318 K; T_{pol}@0.35 M NaCl= 311 K; T_{pol}@0.20 M NaCl= 305 K – data taken from Table 1 of ref. [9]).

Molecular Dynamics calculations

The ΔH°_{dim} value was estimated using $\Delta H^{\circ}_{dim} = < H^{\circ}_{dim} > + < H^{\circ}_{mon} >$, where $<H^{\circ}_{dim}>$ and $<H^{\circ}_{mon}>$ are the system energy averages in the presence of the dimer and of the monomer, respectively. Within the Van't Hoff approximation, i.e. the enthalpy does not change along the

isobar, our estimate at 450K can be compared with the experimental value in the explored temperature range.

The association/dissociation kinetic constants, k_{ass}/k_{diss}, were calculated assuming a diffusive model for the monomer motion. The rate constant at the distance r_0 where the monomers freely diffuse in the solvent is given by:[26]

$$k_{ass} = 4\pi(D_{M,1} + D_{M,2})r_0\mathcal{N}$$

where $\mathcal{N}$ is the Avogadro number and $D_{M,1}$ and $D_{M,2}$ are the DX_{mon} diffusion coefficients.

From k_{ass} and the experimental value of ΔG°_{dim}, k_{diss} was estimated by

$$k_{diss}(T) = k_{ass}(T)e^{\frac{\Delta G^{\circ}_{dim}(T)}{T}}$$

The MD simulation at 300K was used to describe the conformational behaviour of the dimer, whereas the simulation at 450K to estimate the thermodynamics of the dimer-monomer equilibrium. The high temperature MD allows to sample a significant number of monomer/dimer transitions in a reasonable amount of time (200 ns), thus giving the possibility to estimate ΔH°_{dim} and the associated statistical error.

The dimer conformational behaviour at 300K was analysed in terms of the doxorubicin long axis as defined by the vector connecting the midpoints of the C2/C3 and C8/C9 bonds (see Chart 1).

For each MD frame the scalar product between the long axes of the two molecules was calculated to obtain the main orientations between the two molecules, i.e. antiparallel (-1 to -0.5), orthogonal (-0.5 to 0.5) and parallel (0.5 to 1).

The value of the monomer diffusion constant (D_M=2.89·10^{-11} m^2/s) needed to estimate the k_{ass} was taken from the literature,[27] whereas the distance at which the monomers start to freely diffuse was calculated (as 1.5 nm) from the probability distribution of the distance between the monomer centres of mass as provided by the MD simulation at 450K (for further details, see [26]). The same 1.5 nm value was also used in the evaluation of ΔH°_{dim} to define the monomeric state. As expected, the MD simulation at 300K shows the presence of the dimer only.

Using the long DX axis as a measure of the mutual orientation of two DX molecules and the boundary definitions of the three main conformational states (parallel, antiparallel and orthogonal), we found that the antiparallel arrangement is present in more than half of the trajectories (Figure 4). The parallel and the orthogonal orientations were observed in the 15% and 30% of the trajectories, respectively. The mean distance between the centre of mass of the two DX molecules in the dimer is 0.37 nm, in excellent agreement with the literature value of ~0.34 nm based on NMR spectroscopy and molecular mechanics modelling.[14] Making reference to the mode of the distributions obtained by the MD simulations of Figure 4, for the antiparallel DX arrangement a value of -0.94 is obtained while, for the parallel orientation the

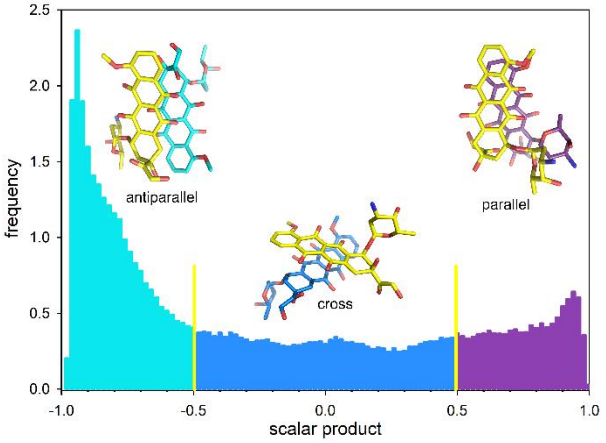

Figure 4 The normalized histogram of the scalar product between the long DX axes (red arrow in Chart 1) as obtained from the 450 K MD simulation. Representative geometries for the antiparallel (-1 to -0.5), orthogonal (cross, between -0.5 and 0.5) and parallel (0.5 to 1) DX arrangements are included as stick representation.

mode is 0.93. These values allow to calculate the most probable angle between the long axes of two adjacent DX molecules. For the two orientations, angles of 160° and 21°, respectively, were obtained. These values are in excellent agreement with the literature data (168° and 15° for the antiparallel and parallel orientations, respectively).[14]

From the MD simulation at 450K, the dimer-monomer thermodynamics was modelled. The value of ΔH°_{dim} at 450 K obtained from the MD simulation (-45±3 kJ/mol), indicating a favourable interaction between the two molecules in water, well compares with our experimental measurements (Figure 3 – Panel B) obtained in the temperature interval 293K-328K.

The kinetic constants associated to the monomer-dimer equilibrium - estimated from the experimental value of K_{dim} and assuming a diffusive model when the distance between the two monomers is greater than 1.5 nm - are $k_{ass} = 6.56 \cdot 10^{8}$ $M^{-1}s^{-1}$ and $k_{diss} = 1.338 \cdot 10^{4}$ s^{-1} yielding a dimer lifetime estimate of 74.7 μs (a direct estimate of the dimer lifetime from the MD simulation at 450K provides a value of ~ 11 ns, compatible with the 150 K temperature increase; see ESI – Figure S1).

Finally, the analysis of the DX structures as sampled by the 450 K MD simulations indicates that its internal degrees of freedom are not significantly affected by the dimer formation, i.e. the distributions of selected dihedral angles of the monomeric form - in line with a previous literature report [28] - do not change upon dimerization (see ESI - Figure S2).

Conclusions

The intrinsic and peculiar fluorescent nature of DX has been exploited in this work to improve our knowledge of the drug association processes, even from a thermodynamic point of view. Also in this instance, the joint use of experimental techniques and MD simulations proved to be the winning strategy to unravel the complex association processes ruling the DX behaviour in solution. Despite its low molar mass, in fact, DX has a chemical complexity that is at the basis of its capability not only to form dimers but also to undergo a T-controlled polymerization that leads to the formation of long chains of DX molecules responsible of the gel properties of the system.[9] The interesting point of the DX dimerization process is that, when the DX concentration is above the CGFC, a substantial independency on ionic strength was found (Figure 3).

The all-atom MD simulations here presented, show mutual orientations of the DX molecules in the dimer closely matching those reported in the literature obtained using ad-hoc restrained MD simulations.[14] In addition, theoretical-computational modelling not only lends support to the experimental findings but also offers an estimate of the residence time of DX molecules in the dimer hardly achievable experimentally even with T-jump apparatus of the last generation.

The thermodynamic parameters derived for the dimerization process both from the fluorescence measurements and from MD calculations here presented are in fairly good agreement with literature data.[14][29] However, at variance with literature data,[10][12] our results point to an independence of the dimerization constant on the NaCl concentration (Figure 3 – Panel B). This point will be the subject of a forthcoming paper, where the dimerization process of DX will be addressed to by means of both fluorescence and MD

simulations by varying in a systematic way the drug concentration below $1 \cdot 10^{-2}$M and the NaCl concentration. The resulting systems will be studied as a function of temperature in order to have access to the thermodynamics of the dimerization process as a function of ionic strength.

Acknowledgement

MG wishes to thank the MIUR (FFABR - Fondo Finanziamento Attività di Base Ricerca - 2017) for financial support.

Bibliography

[1] G. Minotti, P. Menna, E. Salvatorelli, G. Cairo, L. Gianni, Anthracyclines : Molecular Advances and Pharmacologic Developments in Antitumor Activity and Cardiotoxicity, Pharmacol. Rev. 56 (2004) 185–229. doi:10.1124/pr.56.2.6.185.

[2] P. Ma, R.J. Mumper, Anthracycline nano-delivery systems to overcome multiple drug resistance: A comprehensive review, Nano Today. 8 (2013) 313–331. doi:10.1016/j.nantod.2013.04.006.

[3] H. Cortés-Funes, C. Coronado, Role of anthracyclines in the era of targeted therapy, Cardiovasc. Toxicol. 7 (2007) 56–60. doi:10.1007/s12012-007-0015-3.

[4] E. Tasca, A. Del Giudice, L. Galantini, K. Schillén, A.M. Giuliani, M. Giustini, A fluorescence study of the loading and time stability of doxorubicin in sodium cholate/PEO-PPO-PEO triblock copolymer mixed micelles, J. Colloid Interface Sci. 540 (2019) 593–601. doi:10.1016/j.jcis.2019.01.075.

[5] M. Giomini, A. Maria Giuliani, M. Giustini, E. Trotta, Anthracycline gels, Biophys. Chem. 39 (1991) 119–125. doi:10.1016/0301-4622(91)85013-G.

[6] M. Giomini, A.M. Giuliani, M. Giustini, E. Trotta, Anthracycline Gels. II. Spectroscopic study on doxorubicin—lecithin association products, Biophys. Chem. 45 (1992) 31–40. doi:10.1016/0301-4622(92)87021-A.

[7] E. Hayakawa, K. Furuya, T. Kuroda, M. Moriyama, A. Kondo, Studies on the dissolution behavior of doxorubicin hydrochloride freeze-dried product, Chem. Pharmacol. Bullettin. 38 (1990) 3434–3439.

[8] E. Hayakawa, K. Furuya, T. Kuroda, M. Moriyama, A. Kondo, Viscosity study on the self-association of doxorubicin in aqueous solution, Chem. Pharmacol. Bullettin. 39 (1991) 1282–1286.

[9] E. Tasca, M. D'Abramo, L. Galantini, A.M. Giuliani, N.V. Pavel, G. Palazzo, M. Giustini, A Stereochemically Driven Supramolecular Polymerisation, Chem. - A Eur. J. 24 (2018) 8195–8204. doi:10.1002/chem.201800644.

[10] M. Menozzi, L. Valentini, E. Vannini, F. Arcamone, Self-Association of Doxorubicin and Related Compounds in Aqueous Solution, J. Pharm. Sci. 73 (1984) 766–770. doi:10.1002/jps.2600730615.

[11] V. Barthelemy-Clavey, J.-C. Maurizot, J.-L. Dimicoli, P. Sicard, Self-association of

daunorubicin, FEBS Lett. 46 (1974) 5–10.
[12] S.R. Martin, Absorption and Circular Dichroic Spectral Studies on the Self-Association of Daunorubicin, Biopolymers. 19 (1980) 713–721.
[13] S. Eksborg, Extraction of daunorubicin and doxorubicin and their hydroxyl metabolites: Self-association in aqueous solution, J. Pharm. Sci. 67 (1978) 782–785. doi:10.1002/jps.2600670613.
[14] M.P. Evstigneev, V. V. Khomich, D.B. Davies, Self-association of daunomycin antibiotic in various buffer solutions, Russ. J. Phys. Chem. 80 (2006) 741–746. doi:10.1134/S003602440605013X.
[15] I.J. Mclennan, R.E. Lenkinski, I.J. Mclennan, A nuclear magnetic resonance study of the self-association of adriamycin and daunomycin in aqueous solution, Can. J. Chem. 63 (1985) 1233–1238.
[16] M.J. Abraham, T. Murtola, R. Schulz, S. Páll, J.C. Smith, B. Hess, E. Lindah, Gromacs: High performance molecular simulations through multi-level parallelism from laptops to supercomputers, SoftwareX. 1–2 (2015) 19–25. doi:10.1016/j.softx.2015.06.001.
[17] H.J.C. Berendsen, J.P.M. Postma, W.F. VanGunsterenand, J. Hermans, Interaction model for water in relation to protein hydration, in: B.Pullman (Ed.), Intermol. Forces, D. Reidel Publishing Company, 1981: pp. 331–338. doi:10.1.1.460.309.
[18] A.K. Malde, L. Zuo, M. Breeze, M. Stroet, D. Poger, P.C. Nair, C. Oostenbrink, A.E. Mark, An Automated force field Topology Builder (ATB) and repository: Version 1.0, J. Chem. Theory Comput. 7 (2011) 4026–4037. doi:10.1021/ct200196m.
[19] G. Bussi, D. Donadio, M. Parrinello, Canonical sampling through velocity rescaling, J. Chem. Phys. 126 (2007) 014101. doi:10.1063/1.2408420.
[20] S. Del Galdo, P. Marracino, M. D'Abramo, A. Amadei, In silico characterization of protein partial molecular volumes and hydration shells, Phys. Chem. Chem. Phys. 17 (2015) 31270–31277. doi:10.1039/c5cp05891k.
[21] S. Del Galdo, A. Amadei, The unfolding effects on the protein hydration shell and partial molar volume: a computational study, Phys. Chem. Chem. Phys. 18 (2016) 28175–28182. doi:10.1039/c6cp05029h.
[22] B. Hess, H. Bekker, H.J.C. Berendsen, J.G.E.M. Fraaije, LINCS: A linear constraint solver for molecular simulations, J. Comput. Chem. 18 (1997) 1463–1472. doi:10.1002/(SICI)1096-987X(199709)18:12<1463::AID-JCC4>3.0.CO;2-H.
[23] T. Darden, D. York, L. Pedersen, Particle mesh Ewald: An N ·log(N) method for Ewald sums in large systems, J. Chem. Phys. 98 (1993) 10089–10092. doi:10.1063/1.464397.
[24] P. Changenet-Barret, T. Gustavsson, D. Markovitsi, I. Manet, S. Monti, Unravelling molecular mechanisms in the fluorescence spectra of doxorubicin in aqueous solution by femtosecond fluorescence spectroscopy, Phys. Chem. Chem. Phys. 15 (2013) 2937–2944. doi:10.1039/c2cp44056c.
[25] R. Anand, S. Ottani, F. Manoli, I. Manet, S. Monti, A close-up on doxorubicin binding to γ-cyclodextrin: an elucidating spectroscopic, photophysical and conformational study, RSC Adv. 2 (2012) 2346–2357. doi:10.1039/c2ra01221a.
[26] S. Del Galdo, M. Aschi, A. Amadei, In silico characterization of bimolecular electron transfer reactions: The ferrocene–ferrocenium reaction as a test case, Int. J. Quantum Chem. 116 (2016) 1723–1730. doi:10.1002/qua.25212.
[27] P. Agrawal, S.K. Barthwal, R. Barthwal, Studies on self-aggregation of anthracycline drugs by restrained molecular dynamics approach using nuclear magnetic resonance spectroscopy supported by absorption, fluorescence, diffusion ordered spectroscopy and mass spectrometry, Eur. J. Med. Chem. 44 (2009) 1437–1451. doi:10.1016/j.ejmech.2008.09.037.
[28] Y. Tsoneva, H.R.A. Jonker, M. Wagner, A. Tadjer, M. Lelle, K. Peneva, A. Ivanova,

Molecular structure and pronounced conformational flexibility of doxorubicin in free and conjugated state within a drug-peptide compound, J. Phys. Chem. B. 119 (2015) 3001–3013. doi:10.1021/jp509320q.

[29] J.B. Chaires, N. Dattagupta, D.M. Crothers, Selfassociation of daunomycin, Biochemistry. 21 (1982) 3927–3932. doi:10.1021/bi00260a004.